Graphene Terahertz Sources and Amplifiers

Farhan Rana, Paul A. George, Jared H. Strait, and Jahan Dawlaty
Cornell University, Ithaca, NY 14853, USA

***Abstract*—Plasmons in population inverted graphene can experience extremely large gain through the process of stimulated emission at terahertz frequencies. The large gain values and the small plasmon wavelengths can lead to compact terahertz plasmon lasers and amplifiers that are only a few microns in size. We present optical and terahertz spectroscopy results for carrier relaxation and recombination dynamics in graphene and discuss designs for terahertz plasmon lasers and practical schemes for achieving population inversion in graphene.**

I. Introduction And Background

Graphene is a single atomic layer of carbon atoms forming a dense honeycomb crystal lattice [1-5]. Tremendous interest has been generated recently in the electronic properties of graphene in both experimental and theoretical arenas [1-5]. The linear energy dispersion relation of electrons and holes with zero (or close to zero) bandgap results in novel behavior of both single-particle and collective excitations. Plasmons in graphene are charge density waves. Recently, it has been shown that the frequencies of plasmons in graphene at moderate carrier densities (~10^9-10^{11} cm^{-2}) are in the terahertz range [5] (see Fig.3). Unlike plasmons in semiconductor quantum wells, plasmons in graphene are very strongly coupled to the interband electron-hole transitions, leading to strong damping of the plasmons at finite temperatures as plasmons can decay by exciting interband electron-hole pairs [5]. The coupling of the plasmons to interband electron-hole transitions in population inverted graphene layers can lead to plasmon amplification through the process of stimulated emission, as shown in Fig.2 [5].

In graphene, the valence and conduction bands resulting from the mixing of the p_z orbitals are degenerate at the inequivalent K and K' points of the Brillouin zone [5]. Near these points, the conduction and valence band dispersion relations can be written as [5],

$$E_c(\vec{k}) = +v\,\hbar\,k \qquad E_v(\vec{k}) = -v\,\hbar\,k$$

where v is the velocity of the electrons and holes and equals 10^8 cm/s. The complex dispersion of plasmons is given by the equation, $\varepsilon(q,\omega)=0$, where is the longitudinal dielectric function of graphene [5]. In this plasmon mode, the charge density (not the number density) associated with the electrons and the charge density associated with the holes oscillate in-phase. In the random phase approximation (RPA) $\varepsilon(q,\omega)$ can be written as, $\varepsilon(q,\omega)=1-V(q)\Pi(q,\omega)$, where $V(q)$ is the unscreened 2D Coulomb interaction and $\Pi(q,\omega)$ is the electron-hole propagator and included both intraband and interband processes [5]. Expressions for $\Pi(q,\omega)$ are given in [5]. The real part of the interband contribution to the propagator modifies the effective dielectric constant and leads to a modification in the plasmon frequency. The imaginary part of the interband contribution to the propagator incorporates plasmon loss or gain due to stimulated interband transitions. Similarly, the imaginary of the intraband contribution to the propagator describes losses due to carrier intraband scattering. [5]

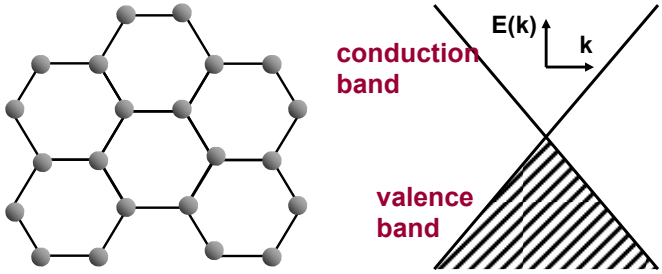

Fig.1: (RIGHT) Graphene lattice. (LEFT) Energy bands of graphene.

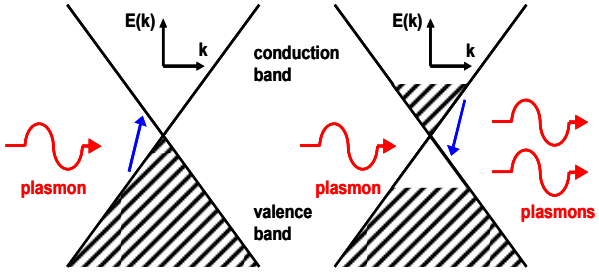

Fig.2: Energy bands of graphene showing stimulated absorption (LEFT) and stimulated emission (RIGHT of plasmons.

Calculated plasmon dispersion at T=77K is shown in Fig.3. Since the plasmon energy $\hbar\omega(q)$ is above the value $v\hbar q$, losses due to intraband absorption of plasmons (Landau damping) are not possible at low terahertz frequencies [5].

Under population inversion conditions, plasmons acquire gain due to stimulated emission of plasmons. At low frequencies (less than 1 THz), the plasmon losses from intraband carrier scattering tend to dominate. At higher frequencies, the net gain becomes positive for electron-hole densities larger than a minimum threshold value. The net plasmon gain values in graphene can exceed 5x10^4 cm^{-1} in the 1-10 terahertz frequency range, for electron-hole densities in the 10^9-10^{11} cm^{-2} range, even when plasmon energy losses due to intraband scattering are considered (see Fig.4). Such high net gain values can allow extremely compact terahertz amplifiers and oscillators that have dimensions in the 1-10 μm range [5]. The large gain values of the plasmons result from two main factors: i) the group velocity of plasmons can be as much as

978-1-4244-2120-6/08/$25.00 ©IEEE.

300 times smaller than the velocity of light, and ii) the plasmon field is tightly confined to the graphene layer.

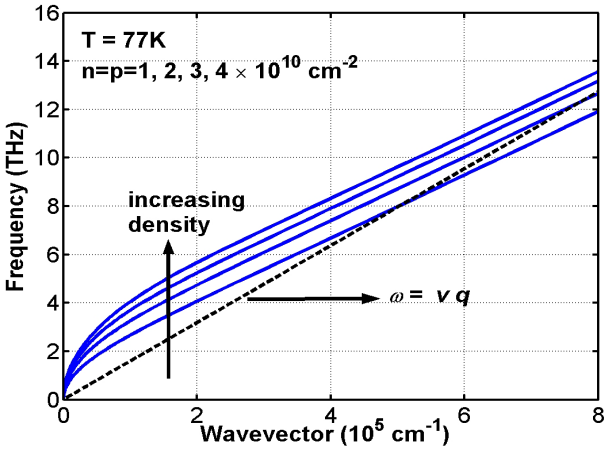

Fig.3: Calculated dispersion of plasmons in graphene at T=77K for different electron and hole densities [5].

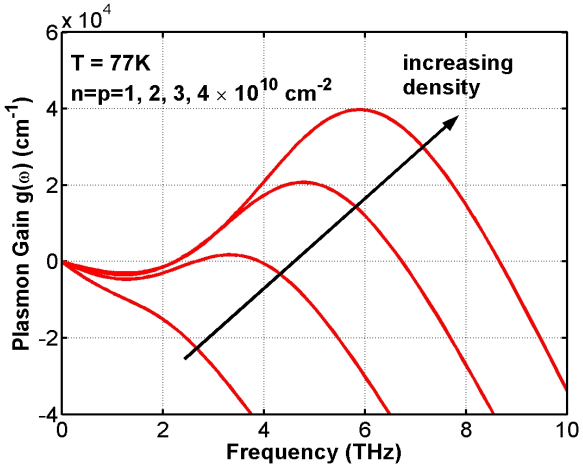

Fig.4: Calculated net plasmon gain in graphene at T=77K for different electron and hole densities. Assumed value for the intraband scattering time is 500 fs [5].

Since plasmons carry charge and current, energy from plasmon oscillators can be coupled out via circuits. We discuss practical designs for graphene terahertz plasmon oscillators and amplifiers. A graphene based terahertz oscillator connected to a load is depicted in Fig.5. The graphene strip itself acts as the plasmon cavity. A transmission-like model can be built for the plasma waves in the graphene strip in which the position dependent potential $V(z)$ and the current $I(z)$ satisfy the equations,

$$V(z) = V_+ e^{i\,q\,z} + V_- e^{-i\,q\,z}$$

$$I(z) = \frac{V_+}{Z_o} e^{i\,q\,z} - \frac{V_-}{Z_o} e^{-i\,q\,z}$$

Where, Z_o is the impedance of the plasmons and has values between a few hundred Ohms to a few kilo-Ohms for a micron wide graphene strip. If z_{ext} is the external impedance as seen by the graphene strip from its two ends (including the ohmic contact impedance), then the condition for oscillation for a graphene strip of length L can be written as [5],

$$\frac{Z_{ext} - 2Z_o}{Z_{ext} - 2Z_o} e^{i\,q\,L} = -1$$

Note that the wavevector q is complex and includes the effects of loss and gain. From the above equation, the required values of the net plasmon gain to achieve oscillation come out to be between 1000 and 3000 cm^{-1}. Since the predicted net gain values are almost 10 times larger in comparison, enough gain-margin is available for extra losses. The impedance of a population inverted graphene strip, as seen from its two ends, can also become negative under population inversion conditions. Therefore, graphene terahertz amplifiers can also be realized (see Fig.5).

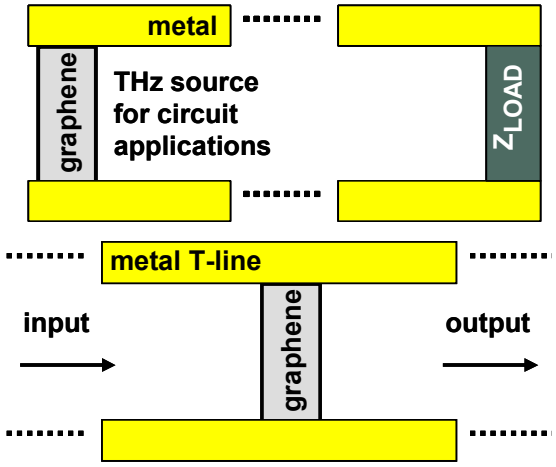

Fig.5: (TOP) Schematic of a graphene terahertz oscillator connected to a load (BOTTOM) Schematic of a graphene terahertz amplifier.

A critical requirement for realizing graphene plasmon terahertz oscillators and amplifiers is the ability to achieve population inversion in graphene. We present experimental results from ultrafast optical-pump and optical-probe and ultrafast optical-pump and terahertz-probe spectroscopy for the carrier interband and intraband dynamics in graphene and demonstrate the feasibility of achieving population inversion via optical and electrical pumping. Results from ultrafast optical-pump and Terahertz-probe spectroscopy at T=300K, reproduced in Fig.6, indicate that carrier recombination times in graphene are carrier density dependent and are in the 5-15 ps range for carrier densities in the 10^{11} cm^{-2} range [7]. These results are in agreement with the theoretical predictions [6]. The measured carrier recombination times are longer than the non-radiative intersubband scattering times in terahertz quantum cascade lasers and suggest that population inversion can be achieved in graphene.

978-1-4244-2120-6/08/$25.00 ©IEEE.

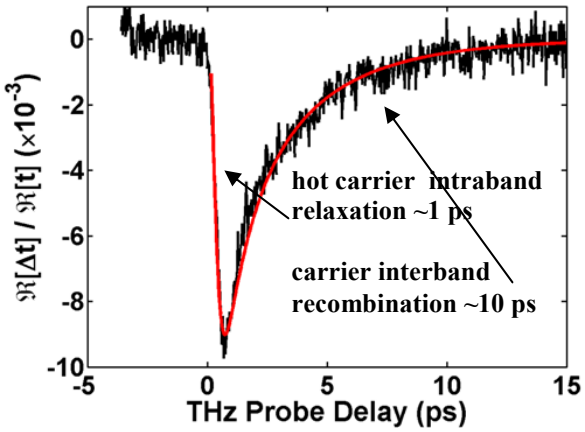

Fig.6: Differential transmission of the THz probe pulse following an optical pulse vs probe delay. The observed dynamics show carrier density dependent recombination times of the photo-excited carriers of around ~5-15 ps.

REFERENCES

[1] K. S. Novoselov et. al., Nature, 438, 197 (2005).
[2] K. S. Novoselov et. al., Science, 306, 666 (2004).
[3] R. Saito, G. Dresselhaus, and M. S. Dresselhaus, *Physical Properties of Carbon Nanotubes*, Imperial College Press, London, UK (1999).
[4] W. De Heer et. al., Science, 312, 1191 (2006).
[5] F. Rana, IEEE Trans. Nanotech., 7, 91 (2008).
[6] J. M. Dawlaty, F. Rana, Appl. Phys. Lett., 92, 042116 (2008).
[7] F. Rana, Phys. Rev. B, 76, 155431 (2007).
[8] P. A. George, J. Strait, J. Dawlaty, S. Shivaraman, Mvs Chandrashekhar, F. Rana, M. G. Spencer, arXiv:0805.4647v3 (2008).

978-1-4244-2120-6/08/$25.00 ©IEEE.